Bifacial dye-sensitized solar cells based on an ionic liquid electrolyte

SEIGO ITO[1,2]*, SHAIK M. ZAKEERUDDIN[2], PASCAL COMTE[2], PAUL LISKA[2], DAIBIN KUANG[2] AND MICHAEL GRÄTZEL[2]

[1]Department of Electrical Engineering and Computer Sciences, Graduate School of Engineering, University of Hyogo, 2167 Shosha, Himeji, Hyogo 671-2280, Japan

[2]Laboratoire de Photonique et Interfaces, École Polytechnique Fédérale de Lausanne, CH-1015, Lausanne, Switzerland

*e-mail: itou@eng.u-hyogo.ac.jp

Published online: 19 October 2008; doi:10.1038/nphoton.2008.224

Solar energy is a promising solution to global energy-related problems because it is clean, inexhaustible and readily available. However, the deployment of conventional photovoltaic cells based on silicon is still limited by cost, so alternative, more cost-effective approaches are sought. Here we report a bifacial dye-sensitized solar cell structure that provides high photo-energy conversion efficiency (∼6%) for incident light striking its front or rear surfaces. The design comprises a highly stable ruthenium dye (Z907Na) in combination with an ionic-liquid electrolyte and a porous TiO_2 layer. The inclusion of a SiO_2 layer between the electrodes to prevent generation of unwanted back current and optimization of the thickness of the TiO_2 layer are responsible for the enhanced performance.

New schemes for generating electricity are necessary in order to help solve global problems such as energy shortage, pollution, population growth and shortages of food and water. Solar energy is a particularly promising solution because it is a clean source of energy, inexhaustible, and can be used anywhere in the world. However, the deployment of commercially available silicon solar cells is currently limited by their relatively high fabrication costs. To achieve a short cost payback period (<10 years) and promote wider deployment of photovoltaic technology it is necessary to design and produce solar cells that are more cost effective. For example, the target of the New Energy and Industrial Technology Development Organization (NEDO, Japan) is to fabricate a 1 W solar cell with a cost of 50 yen, calculated on the basis of the Kyoto Protocol (overview of 'PV Roadmap Toward 2030 (PV2030)'; June 2004, NEDO).

One approach to reducing costs is to use bifacial solar cells[1–4], which are capable of converting incident sunlight to electricity at the front and rear faces of the cell, thus allowing smaller sized cells to generate more electricity. It has been shown that properly installed bifacial modules can produce up to 50% more electric power by collecting albedo radiation from the surroundings[2,3]. Although the bifacial approach has been investigated since 1966 (ref. 1), it has attracted particular interest in recent years, and bifacial polycrystalline silicon solar cells are now manufactured by Hitachi Electronics[4].

However, because of their high cost, silicon bifacial cells are still not widely used in the commercial market despite their advantages of using reflected light from the surroundings or from static concentrators. The high manufacturing and material costs of silicon solar cells has recently motivated several research groups to develop different kinds of bifacial solar cells based on alternative materials such as CdTe (ref. 5), CuInGaSe (refs 6,7) and GaAs (ref. 8).

An alternative approach is the use of dye-sensitized solar cell (DSC) technology[9–11]. As well as being potentially cost-effective to fabricate, additional advantages of these cells include the high availability and non-toxicity of the main component, TiO_2, which is used in paints, cosmetics and healthcare products. Following the report of Matsumura and Tsubomura regarding a DSC containing a combination of a porous zinc oxide electrode with a sensitizing dye (1% conversion efficiency)[12,13], significant effort has been invested into realising DSCs. Researchers at École Polytechnique Fédérale de Lausanne, Sharp and the National Institute of Advanced Science and Technology (AIST) have reported DSCs with power conversion efficiencies of 10.4, 11.1 and 10.5%, respectively[14–16], with this performance subsequently confirmed by governmental institutes in USA and Japan. However, these high-efficiency DSCs were composed of volatile solvent electrolytes, which are therefore not suitable for outdoor conditions. As a result of further investigations regarding stability, we recently reported a stable DSC with a 6% conversion efficiency using a solvent free ionic liquid (IL) electrolyte[17], which has the benefits of thermal stability, non-flammability, high ionic conductivity, negligible vapour pressure, a wide electrochemical window and non-toxicity[18].

Although there have been some reports of DSCs in rear-side irradiation systems[19,20], here we report an IL electrolyte bifacial DSC based on porous TiO_2. Performance is enhanced by the use of a porous SiO_2 layer between the TiO_2 and platinum electrodes and careful optimization of the TiO_2 thickness. The structure of the bifacial cell is shown in Fig. 1a. Usually, if an IL electrolyte[21,22] is used in the cell, the efficiency will be substantially lowered due to the dark colour inherent to substances with high I_3^- concentrations and the low diffusion length of I^-/I_3^- in viscous IL electrolytes. Here, we optimise the components of a bifacial DSC system (that is suitable for

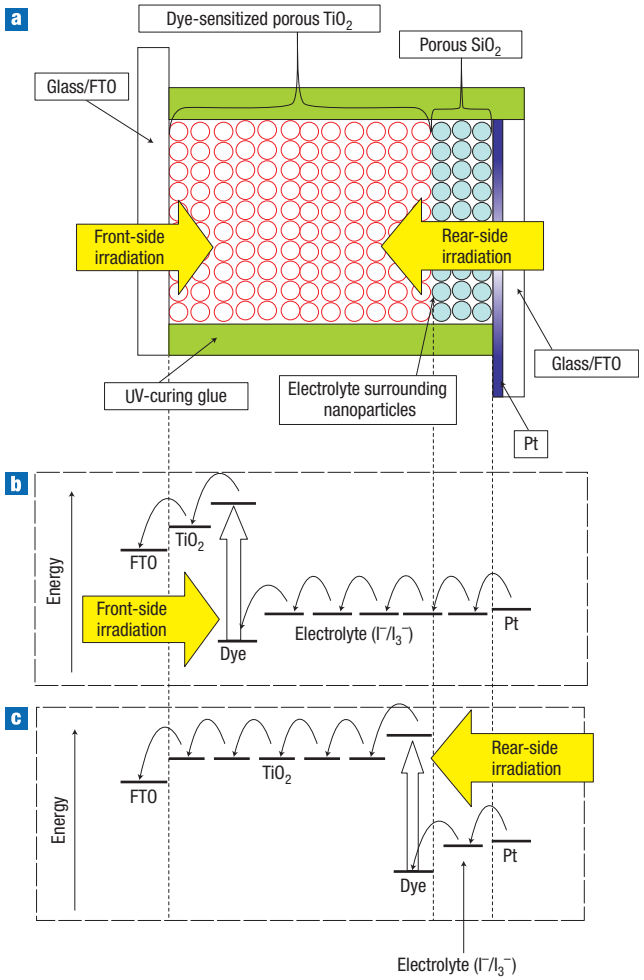

Figure 1 Design of the bifacial DSC. a, Structure of the cell. **b**,**c**, Schemes representing electron flow with irradiation from the front (**b**) and rear (**c**), respectively. The thickness of the dye-sensitized TiO_2 porous electrode was varied from 4.7 to 22.9 μm. The thickness of the SiO_2 porous layer was 3 μm. The dye-sensitized TiO_2 porous electrode on F-doped tin oxide (FTO) was in the shape of a circle of 6 mm diameter. The irradiated light can be absorbed by the dyes at the side of irradiation (front or rear).

outdoor use) in order to enhance the photovoltaic performance in the presence of an IL electrolyte. The porous SiO_2 layer can optically channel the light to the DSC by reducing the optical density of the I^-/I_3^- electrolyte. Moreover, the dye is not adsorbed onto the SiO_2 surface. Another important advantage of the porous SiO_2 layer is its function as an electrical insulator for the platinum counter electrode.

The bifacial cell shown in Fig. 1a is composed of F-doped tin oxide (FTO)/glass substrates coated with mesoporous TiO_2. The mesoporous TiO_2 layer is sensitized with ruthenium dye (Z907Na) and functions as a photoactive electrode, and a porous SiO_2 layer acts as a spacer between the photo anode and the counter electrode (a platinum layer a few nanometres thick). The structure is filled with an IL electrolyte. The cell is assembled by using a UV-curing glue, which enables free control of the distance between the working electrode and the counter electrode and ensures direct contact between the porous SiO_2 layer and the platinum counter electrode. The direct contact reduces the bulk of the electrolyte and increases the amount of incident light for the rear-side irradiation of the dye-sensitized mesoporous TiO_2 layer, which is important because photon absorption by the electrolyte containing I_3^- is significant[20,23].

Figure 1b,c shows a schematic representation of the electron dynamics for the cases of front- and rear-side irradiation, respectively. In a 2.4-μm-thick dye-sensitized porous TiO_2 layer, 50% of the incident light is absorbed in accordance with the Beer–Lambert law[23]. Hence, photo-excitation in the porous TiO_2 electrode occurs mostly around the side being irradiated. In the case of front-side irradiation, the electron path in the TiO_2 conduction band is shorter, and the hole paths in the electrolyte, which span from the reduced dye to the platinum counter electrode, are longer in comparison to those for the case of rear-side irradiation. This effect can reduce the difference between the conversion efficiencies for front- and rear-side irradiation, resulting in high performance and enabling cost-effective application in large-scale solar power generation systems.

In order to improve the DSC performance, optimization of the thickness of the porous TiO_2 layer is very important because the photovoltaic characteristics exhibit significant variation depending on the thickness of the porous TiO_2 (refs 20,24). In this report, we used DSCs containing semitransparent films with 42-nm-diameter TiO_2 particles, resulting in high conversion efficiency[20] compatible with scatter layers[24]. Figure 2 shows the variations in the photovoltaic characteristics of bifacial DSCs depending on the thickness of the dye-sensitized porous TiO_2 layer.

The open-circuit photovoltage (V_{OC}) decreased linearly with the increase in TiO_2 film thickness (Fig. 2a). The slope of V_{OC} for front-side irradiation was steeper than that for rear-side irradiation. We speculate that the relationship between the slope of V_{OC} and the porous TiO_2 thickness might imply an inhomogeneous density of the excited dye in the porous TiO_2 layer. In the case of front-side irradiation (Fig. 1b), the dye is capable of absorbing 50% of the incident light in a 2.4-μm-thick dye-sensitized porous TiO_2 layer[23], resulting in a dye-excited area on the FTO side and a non-excited area on the IL side. The electrons injected from the dye to the TiO_2 layer are averaged homogeneously from the FTO side to the IL side in the porous TiO_2 layer under open-circuit conditions[25,26]. Therefore, increasing the thickness leads to increasing the non-excited area, which lowers V_{OC} further after averaging the electron density in the non-excited area. On the other hand, in the case of rear-side irradiation (Fig. 1c), the incident light is filtered by the iodide electrolyte[19], resulting in blocking the blue-light region and passing the red-light region. Even though the ruthenium dye in the DSC has a lower excitation coefficient in the red-light region than in the blue-light region, red light can penetrate the dyed nanocrystalline TiO_2 layer and provide homogeneous excitation in the layer. For rear-side irradiation, therefore, the additional TiO_2 layer can induce excitation of the dye with red light, after which the additional layer might have a smaller effect on the deterioration of V_{OC} after averaging the electron density. This may explain the difference from the case with front-side illumination. An advanced study on electron dynamics (impedance, electron extraction and other parameters) aimed at elucidating the dependence of the variation in V_{OC} on the thickness of the nanocrystalline TiO_2 layer will be presented in a forthcoming paper.

The maximum short-circuit photocurrents (J_{SC}) corresponding to front- and rear-side irradiation were obtained with 19- and 16-μm-thick films, respectively (Fig. 2b). J_{SC} for any front-side irradiation condition is larger than that for the same condition with rear-side irradiation because the counter electrode and the I^-/I_3^- electrolyte absorb most of the light up to the 400 nm

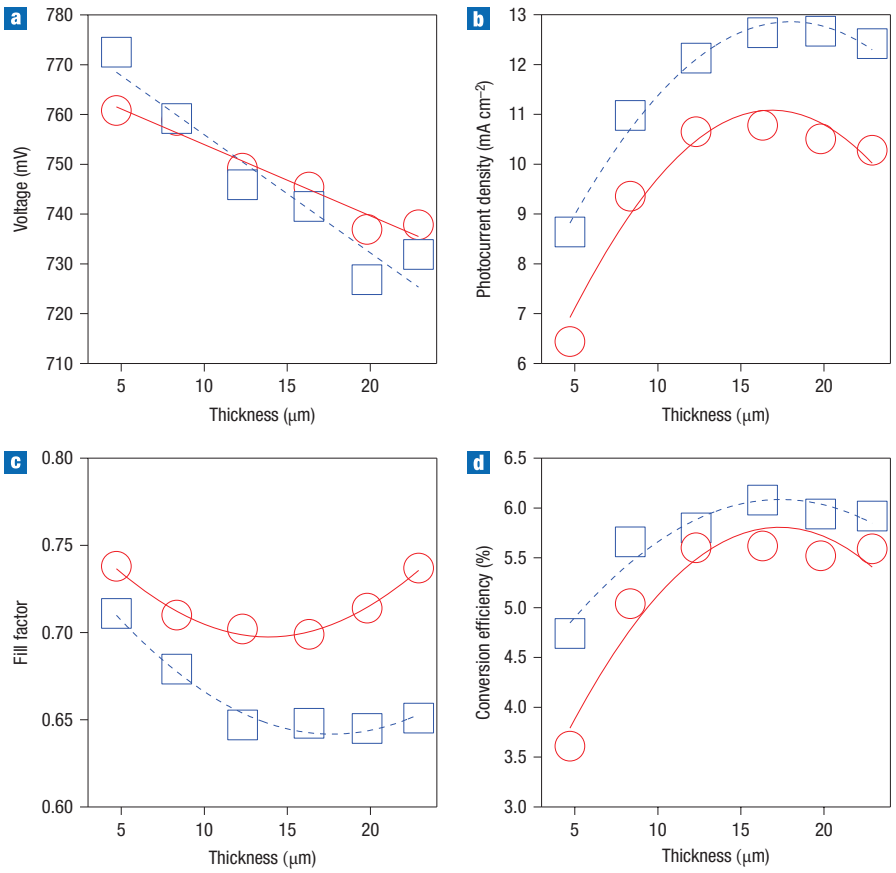

Figure 2 Relationship between the photovoltaic characteristics of bifacial DSCs with TiO_2/SiO_2 (3 μm thick) porous electrodes and the thickness of the porous TiO_2 electrodes. Blue squares and red circles represent front- and rear-side irradiation, respectively. **a**, Open-circuit photovoltage, V_{OC}. **b**, Short-circuit photocurrent density, J_{SC}. **c**, Fill factor, FF. **d**, Photopower energy conversion efficiency, η. The lines represent best fit.

region[20]. By using a mesoporous TiO_2 film thicker than 19 μm, J_{SC} was decreased due to the diffusion limitation of the redox couple (I^-/I_3^-) in the IL (ref. 24).

The fill factor (FF), which is the ratio of the maximum power point divided by the V_{OC} and the J_{SC}, has valleys at 17 and 14 μm for front- and rear-side irradiation, respectively (Fig. 2c). Owing to the series resistance of the DSC, higher J_{SC} values provide low FF values. Because J_{SC} is higher in the case of front-side irradiation than in the case of rear-side irradiation, the FF for front-side irradiation was smaller than that for rear-side irradiation. The variations in the thickness of the porous TiO_2 layer cause valleys in the FF. The magnitude of the variation of both V_{OC} and FF was 5%, whereas the J_{SC} varied by over 50%. Consequently, the energy conversion efficiency (η) had a peak value for the 16-μm-thick TiO_2 film (Fig. 2d), in which the difference in the conversion efficiency between front- and rear-side irradiation was 10%. Therefore, a TiO_2 layer with a thickness of 16 μm was used in this study.

Figure 3a shows the photocurrent/voltage (I–V) curves of the DSCs corresponding to front- and rear-side irradiation with and without a porous SiO_2 spacer. The photovoltaic characteristics are summarized in Table 1. Here, the conversion efficiencies for front- and rear-side irradiation are very close (Fig. 2) due to the optimization of the porous TiO_2 electrode thickness. In addition, the porous SiO_2 spacers improve the values of J_{SC}, resulting in an improvement in the conversion efficiencies.

Figure 3b shows the incident photon-to-current efficiency (IPCE) data. If a polymer spacer is used to control the distance between the porous electrode and the platinum counter electrode instead of the UV-curing glue, the bulk of the electrolyte between the electrodes can be increased. The I^-/I_3^- electrolyte exhibits significant absorption of visible light with a shorter wavelength[20,23]. The IPCE response in the shorter wavelength region decreases as the thickness of the spacer increases, resulting in a decrease of the photocurrent. Therefore, in order to reduce the bulk electrolyte thickness, a liquid-type UV-curing glue was used to achieve high-efficiency bifacial DSCs.

In addition, electrical impedance spectroscopy was performed in order to investigate the performance of the bifacial DSCs (Fig. 4a,b). R_s, CPE and R represent series resistance, constant phase element (equivalent electrical circuit component that models the behaviour of a double layer, an imperfect capacitor) and resistance, respectively. Each peak was analysed by using a simple electrical circuit model (Fig. 4b, inset) and Table 2 summarizes the results. Each intercept on the x-axis at the left edge of the Cole–Cole plots (Fig. 4a) is the same. Hence, the series resistances (R_s) of the DSCs take a constant value of 4.6 Ω.

Comparing the front- and rear-side irradiation cases, the semicircles of the Cole–Cole plots of $R_{Pt/EL}$ (left-side semicircles in Fig. 4a) were the same. The semicircle of $R_{TiO_2/EL}$ (the central semicircle in Fig. 4a) for rear-side irradiation was larger than that for front-side irradiation, indicating that the electron path length

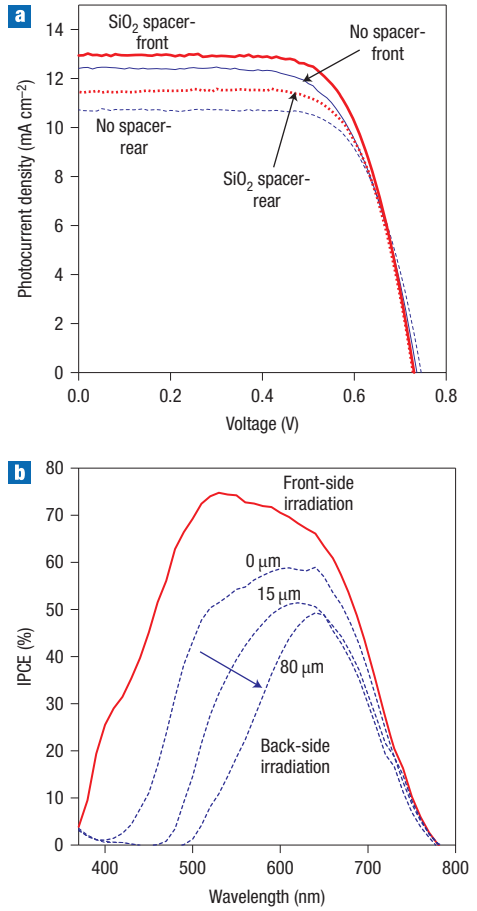

Figure 3 Experimental results of photovoltaic characteristics of DSCs with a porous TiO_2 (16 μm thick) layer. a, Photo *I*–*V* curves of DSCs with (thick line) and without (thin line) a porous SiO_2 layer under front- (solid line) and rear-side irradiation (broken line). **b**, Incident photon-to-current efficiency (IPCE) spectra of DSCs with TiO_2/SiO_2 electrodes for front- (solid line) and rear-side irradiation with different spacers (broken lines). Inset numbers represent the distances between the top of the porous SiO_2 layer and the platinum counter electrode in each case.

Table 1 Photovoltaic characteristics of bifacial DSCs, with and without a porous SiO_2 layer, for rear- and front-side irradiation. The photoactive area was 0.269 cm^2.

	TiO_2		TiO_2/SiO_2	
	Front	Rear	Front	Rear
J_{SC} (mA cm^{-2})	12.6	10.78	13.1	11.6
V_{OC} (V)	0.736	0.754	0.730	0.728
FF	0.662	0.699	0.685	0.705
η (%)	6.13	5.62	6.54	5.96

V_{OC}, open-circuit photovoltage; J_{SC}, short-circuit photocurrent density; FF, fill factor; η, photopower energy conversion efficiency.

in the porous TiO_2 electrode is longer for rear-side irradiation. The semicircles of R_{EL} (right-side semicircles in Fig. 4a) for front-side irradiation were larger than those for rear-side irradiation. This suggests that for front-side irradiation, the redox carrier diffusion path is longer that that for rear-side irradiation. For front-side irradiation, the electron excitation is closer to the FTO substrate, and thus the resulting holes must hop between the elements of the redox couple (I^-/I_3^-) and pass the long distance (15 μm) in the narrow TiO_2 pore (d = 40 nm) from the reduced dye to the platinum counter electrode. On the other hand, for rear-side irradiation, the distance that the electrons must cover is shorter because the excitation dye layer is closer to the platinum counter electrode. Hence, the resistance of the electrolyte decreased for rear-side irradiation.

The porous SiO_2 layer on top of the porous TiO_2 layer has a significant effect on the photo *I*–*V* characteristics (Fig. 3a, Table 1). This porous SiO_2 layer can act as a rigid matrix for the bulk of the electrolyte. J_{SC} increased for both front- and rear-side irradiation when a porous SiO_2 layer was used as a spacer, as shown in Fig. 3a. Others[27,28] have explained that the J_{SC} enhancement indicates enhancement of the electrolyte conductivity attributable to the porous SiO_2 layer. In Fig. 3a, however, R_{EL} was increased by the addition of the porous SiO_2 layer, indicating the restriction of the movement of the redox couple within the electrolyte. This difference may arise from the presence of the bulk of the IL electrolyte by the film spacer between the TiO_2 and platinum electrodes in the DSCs of refs 27 and 28, because the bulk of the IL electrolyte in the case where the film spacer was used possesses higher resistivity than the IL electrolyte in a porous film. No spacer was used in the case presented in Fig. 3a, where the bulk of the electrolyte was missing. Because the SiO_2 layer simply increased the resistance of the electrolyte located between the TiO_2 and platinum electrodes, R_{EL} was increased by adding the SiO_2 layer.

We can interpret the impedance results on the basis of the partial rear current. Some electrons are able to move from TiO_2 to platinum because TiO_2 attaches on platinum directly without a porous SiO_2 layer as a spacer. The Bode plots (Fig. 4b) explain the effect of the partial rear current. Upon comparing the DSCs with and without a porous SiO_2 layer, it is evident that the peaks of $R_{EL/Pt}$ and R_{EL} are notably shifted, although the peaks of $R_{TiO_2/EL}$ in the Bode plots are not changed. The shift of the $R_{EL/Pt}$ and R_{EL} peaks in the Bode plots suggests a change in the electron lifetime[29]. Therefore, in this case, it was considered that the electron recombination path arises directly from the dye TiO_2 to the platinum due to the direct contact between them. However, when using the porous SiO_2 layer, the dye TiO_2 and the platinum electrode are separated from each other, which eliminates the direct path formed by the direct contact between the dye TiO_2 and the platinum electrode. Therefore, a larger number of electrons can reach FTO when a porous SiO_2 layer is used than in the case with no SiO_2 layer, resulting in a high J_{SC} value and the enhancement of the photovoltaic effect (Fig. 3a).

Figure 4c shows the dynamics of the short-circuit photocurrent at different light intensities. In the case of front-side irradiation, photocurrent deterioration was observed when the light intensity was increased. However, rear-side irradiation did not display such deterioration on the plateau of photocurrent response. A linear response was observed in correspondence to the intensity of the illumination, which is indicated by the fact that the height of the plateau of the photocurrent responses was scaled to 1 sun by multiplication with the attenuation factors. Therefore, under 100% sun illumination, the difference between the photocurrents for front- and rear-side incident irradiation was small, resulting in similar efficiencies (Fig. 2d).

This effect can be explained using Fig. 1. Because the dye is excited closer to the FTO substrate in the case of front-side irradiation (Fig. 1b), the resulting holes must hop between the redox couple (I^-/I_3^-) and cross the long distance in the narrow pores (d = 40 nm) of the porous TiO_2 layer in order to reach the platinum counter electrode. The accumulated carriers in the

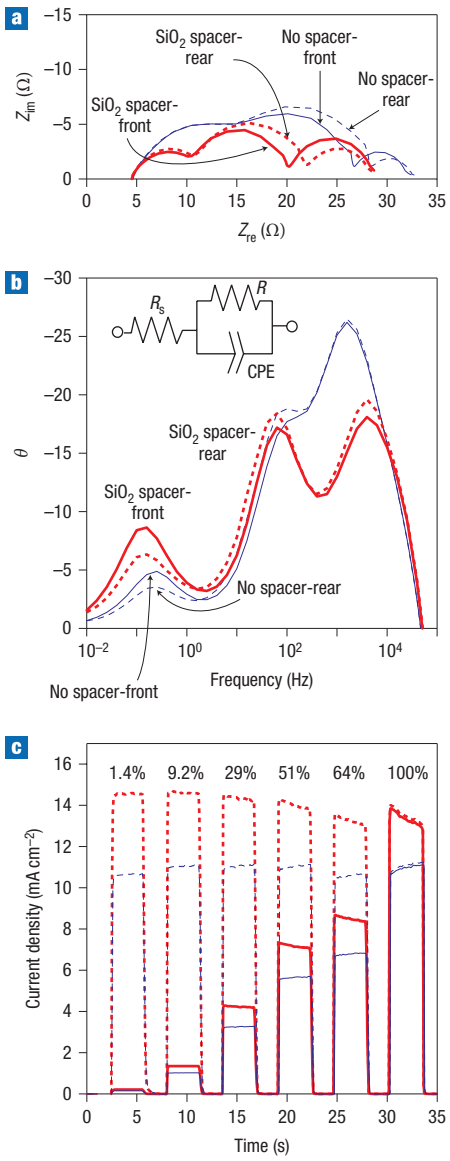

Figure 4 Electrical characteristics of the bifacial DSC. a,**b**, Cole–Cole plots (**a**) and Bode plots (**b**) for DSCs with (thick lines) and without (thin lines) a porous SiO_2 layer (3 μm thickness) on a porous TiO_2 layer (16 μm thickness) for front- (solid lines) and rear-side (broken lines) irradiation. **c**, Current dynamics of the short-circuit photocurrent density (solid lines) with irradiation from the front (bold line) and rear (thin line). Inset numbers represent the illumination power. Broken lines represent photocurrents scaled to 1 sun by multiplication with the attenuation factors. Platinum counter electrodes and porous layers were attached directly without a spacer between the electrodes.

IL can become retarded in the narrow pores, resulting in the deterioration of the photocurrent by the limitation of redox diffusion. On the other hand, for rear-side irradiation (Fig. 1c), the distance covered by the electrons in the redox couples is short because the dye excitation occurs closer to the platinum counter electrode. Therefore, the resistance of the electrolyte in the case of rear-side irradiation becomes small and the deterioration becomes negligible (Fig. 4c). Coincidentally, the results of the analysis regarding current dynamics are in good agreement with the results of the impedance analysis (Fig. 4a,b).

Table 2 Impedance resistance elements in bifacial DSCs, with and without a porous SiO_2 layer, for rear- and front-side irradiation and open-circuit conditions.

Resistance	TiO_2		TiO_2/SiO_2	
	Front	Rear	Front	Rear
$R_{EL/Pt}$	15.2	14.9	7.12	7.54
$R_{TiO2/EL}$	17.8	19.5	10.8	12.4
R_{EL}	5.95	4.89	8.67	7.11

The subscripts of resistance R indicate the interfaces or the bulk of materials that act as the electron paths: $R_{EL/Pt}$, interface resistance between electrolyte and platinum; $R_{TiO_2/EL}$, interface resistance between TiO_2 and electrolyte; and R_{EL}, resistance of electrolyte. Units are ohms.

In conclusion, bifacial DSC structures containing an IL electrolyte exhibited similarly high photovoltaic performance with respect to both front- and rear-side irradiation. The advantages of this arrangement are threefold: (1) reduction of the thickness of the bulk electrolyte by the use of a porous SiO_2 layer and a UV-curing glue; (2) elimination of the charge recombination between TiO_2 and platinum by using the porous SiO_2 layer; and (3) control of the dye excitation induced on the porous TiO_2 layer. Although standard DSCs are transparent and can be used as bifacial solar cells, the ratio of the respective efficiencies for front- and rear-side irradiation are usually very different, with a ratio of 0.63 (ref. 20). In contrast, for the bifacial DSCs described in this report that figure is increased to a factor of 0.91.

For bifacial solar cells, there are two paths for potential application. One arises where bifacial solar cells are used with static solar concentrators, resulting in a 50% increase in electric power generation[2,3]. For DSCs, the designed concentrator can be set between the cells in a module package. The other application arises where bifacial solar cells are set in a standing position with their surfaces facing east and west, generating high electricity both in the morning and the evening[4]. The combination of these two approaches is promising, and relevant experiments should be performed in the future using a large DSC module.

METHODS

For the preparations of stable DSCs, a ruthenium dye (Z907Na) was synthesized using a typical one-pot synthesis and then purified by column chromatography (LH-20, Sephadex)[30]. For the synthesis of TiO_2 particles[31], titanium(IV) isopropoxide (162 ml/0.5 mol, Fluka) was rapidly added to distilled water (290 ml/15.5 mol), stirred for 1 h, filtered using a glass frit, and washed three times with 50 ml distilled water. The resulting filter cake was added to a Teflon-lined titanium autoclave containing 30 ml of 0.6 M tetramethylammonium hydroxide (Fluka) to form a white slurry with a pH of 13. Peptization in the presence of tetramethylammonium hydroxide occurred after heating the product at 100 °C for 6 h. The suspensions resulting from the peptization were hydrothermally treated in an autoclave at temperatures around 240 °C for 4.5 h. The pH of the resultant colloidal suspension was measured at between 13 and 13.5. The procedure for the preparation of TiO_2 paste by mixing with terpineol and ethylcellulose was the same as the procedure using TiO_2 dispersion, as described previously[32]. A bottle of SiO_2 dispersion ($d = 600$ nm), supplied by Catalysts & Chemicals Ind. Co., was converted to a screen-printing paste by mixing with terpineol and ethylcellulose in the same procedure as that used for the TiO_2 paste.

For the preparation of the DSC working electrodes, FTO-glass plates (TEC 15 Ω/□, 2.2 mm thickness, Pilkington) were used. The details of the fabrication scheme are described in a previous report[32]. After the second $TiCl_4$ treatment of the porous TiO_2 electrodes, the SiO_2 paste was coated onto the porous TiO_2 layer by screen printing and heated at 450 °C for 30 min in air. After cooling to 80 °C, the TiO_2/SiO_2 electrode was immersed in a 0.5 mM Z907Na dye solution in a mixture of acetonitrile and *tert*-butyl alcohol (volume ratio, 1:1) and kept at room temperature overnight to complete the uptake of the sensitizer.

For the preparation of the DSC platinum counter electrodes, FTO-glass plates (TEC 15 Ω/□, 2.2 mm thickness, Pilkington) were used. Details of the fabrication scheme are described in a previous report[32].

The dye-covered TiO_2 electrode and the platinum counter electrode were assembled into a sandwich-type cell and sealed with a UV-curing glue (31X-101, Three Bond) by irradiation with UV light. The UV-curing glue was applied using screen printing and a high-pressure mercury lamp (Ushio). In order to achieve direct contact between the porous electrodes (TiO_2 and/or SiO_2/TiO_2) and the platinum counter electrode, a 1 kg glass plate was placed on the cell before curing, and UV light was irradiated through the plate for 30 s. In order to prevent the UV radiation from causing dye deterioration, a small piece of aluminium adhesive tape was placed on the 1 kg glass plate in such a way as to cast a shadow onto the TiO_2 electrode. Furthermore, in order to control the distance between the porous SiO_2/TiO_2 and the platinum counter electrodes, polymer films were used as spacers in the UV-curing glue.

A drop of the electrolyte (0.5 M *N*-methylbenzimidazole, 0.2 M I_2 and 0.1 M guanidinium thiocyanate in a mixture of 1-propyl-3-methylimidazolium iodide/1-ethyl-3-methylimidazolium thiocyanate, 13:7 vol. ratio)[21,22] was driven into the cell by the phenomenon of vacuum filling. The details of the fabrication scheme are described in a previous report[32].

The power of an AM 1.5 solar simulator (100 mW cm^{-2}) was calibrated using a reference silicon photodiode equipped with an infrared cutoff filter (KG-3, Schott) in order to reduce the mismatch between the simulated light and AM 1.5 in the region of 350–700 nm to less than 2% (refs 15,33). The *I*–*V* curves were obtained by the application of an external bias to the cell and by measuring the generated photocurrent with a digital source meter (2400, Keithley). Losses due to light reflection were eliminated by using a self-adhesive fluorinated polymer film (Arctop, Asahi Glass), which also served as a 380-nm UV cutoff filter. Masks made of black plastic tape were attached on the Arctop filter to reduce the scattering of light[34].

Received 10 March 2008; accepted 22 September 2008; published 19 October 2008.

References

1. Mori, H. Radiation energy transducing device. US patent 3,278,811 (1966).
2. Hübner, A., Aberle, A. G. & Hezel, R. Cost-effective bifacial silicon solar cells with 19% front and 18% rear efficiency. *Conf. Proc. 25th PVSC*, 13–17 May 1996, 489–492 (IEEE, Washington, DC).
3. Hübner, A., Aberle, A. G. & Hezel, R. Novel cost-effective bifacial silicon solar cells with 19.4% front and 18.1% rear efficiency. *Appl. Phys. Lett.* **70,** 1008–1010 (1997).
4. Uematsu, T. *et al.* Development of bifacial PV cells for new applications of flat-plate modules. *Solar Energy Mater. Solar Cells* **75,** 557–566 (2003).
5. Khrypunov, G. *et al.* Recent development in evaporated CdTe solar cells. *Solar Energy Mater. Solar Cells* **90,** 664–677 (2006).
6. Rostan, P. J. *et al.* Formation of transparent and ohmic ZnO:Al/$MoSe_2$ contacts for bifacial Cu(In,Ga)Se_2 solar cells and tandem structures. *Thin Solid Films* **480–481,** 67–70 (2005).
7. Nakada, T. *et al.* Novel device structure for Cu(In,Ga)Se_2 thin film solar cells using transparent conducting oxide back and front contacts. *Solar Energy* **77,** 739–747 (2004).
8. Schermer, J. J. *et al.* Photon confinement in high-efficiency, thin-film III–V solar cells obtained by epitaxial lift-off. *Thin Solid Films* **511–512,** 645–653 (2006).
9. O'Regan, B. & Grätzel, M. A low-cost, high-efficiency solar cell based on dye-sensitized colloidal TiO_2 films. *Nature* **353,** 737–739 (1991).
10. Grätzel, M. Photoelectrochemical cells. *Nature* **414,** 338–344 (2001).
11. Smestad, G., Bignozzi, C. & Arazzi, R. Testing of dye-sensitized solar cells I: Experimental photocurrent output and conversion efficiencies. *Solar Energy Mater. Solar Cells* **32,** 259–272 (1994).
12. Tsubomura, H., Matsumura, M., Noyamaura, Y. & Amamiya, T. Dye sensitized zinc oxide: Aqueous electrolyte: Platinum photocell. *Nature* **261,** 402–403 (1976).
13. Matsumura, M. PhD thesis, Osaka University, Japan (1979).
14. Nazeeruddin, Md. K. *et al.* Engineering of efficient panchromatic sensitizers for nanocrystalline TiO_2-based solar cells. *J. Am. Chem. Soc.* **123,** 1613–1624 (2001).
15. Chiba, Y. *et al.* Dye-sensitized solar cells with conversion efficiency of 11.1%. *Jpn J. Appl. Phys.* **45,** L638–L640 (2006).
16. Wang, Z. S., Yamaguchi, T., Sugihara, H. & Arakawa, H. Significant efficiency improvement of the black dye-sensitized solar cell through protonation of TiO_2 films. *Langmuir* **21,** 4272–4276 (2005).
17. Kuang, D. *et al.* Stable, high-efficiency ionic-liquid-based mesoscopic dye-sensitized solar cells. *Small* **3,** 2094–2102 (2007).
18. Ionic Liquids IIIA. *Fundamentals, Progress, Challenges and Opportunities: Properties and Structure* (eds Rogers, R. D. & Seddon K. R.) (ACS Symposium Series, 2005).
19. Kang, M. G. *et al.* A 4.2% efficient flexible dye-sensitized TiO_2 solar cell using stainless steel substrate. *Solar Energy Mater. Solar Cells* **90,** 574–581 (2006).
20. Ito, S. *et al.* High-efficiency (7.2%) flexible dye-sensitized solar cells with Ti-metal substrate for nanocrystalline-TiO_2 photoanode. *Chem. Commun.* 4004–4006 (2006).
21. Mohmeyer, N. *et al.* An efficient organogelator for ionic liquids to prepare stable quasi-solid-state dye-sensitized solar cells. *J. Mater. Chem.* **16,** 2978–2983 (2006).
22. Kuang, D. *et al.* High molar extinction coefficient heteroleptic ruthenium complexes for thin film dye-sensitized solar cells. *J. Am. Chem. Soc.* **128,** 4146–4154 (2006).
23. Kubo, W. *et al.* Photocurrent-determining processes in quasi-solid-state dye-sensitized solar cells using ionic gel electrolytes. *J. Phys. Chem. B* **107,** 4374–4381 (2003).
24. Ito, S. *et al.* High-efficiency organic-dye-sensitized solar cells controlled by nanocrystalline-TiO_2 electrode thickness. *Adv. Mater.* **18,** 1202–1205 (2006).
25. Würfel, U., Wagner, J. & Hinsch, A. Spatial electron distribution and its origin in the nanoporous TiO_2 network of a dye solar cell. *J. Phys. Chem. B* **109,** 20444–20448 (2005).
26. Fabregat-Santiago, F. *et al.* Influence of electrolyte in transport and recombination in dye-sensitized solar cells studied by impedance spectroscopy. *Solar Energy Mater. Solar Cells* **87,** 117–131 (2005).
27. Usui, H., Matsui, H., Tanabe, N. & Yanagida, S. Improved dye-sensitized solar cells using ionic nanocomposite gel electrolytes. *J. Photochem. Photobiol. A* **164,** 97–101 (2004).
28. Berginc, M. *et al.* Ionic liquid-based electrolyte solidified with SiO_2 nanoparticles for dye-sensitized solar cells. *Thin Solid Films* **516,** 4645–4650 (2008).
29. Kern, R. *et al.* Modeling and interpretation of electrical impedance spectra of dye solar cells operated under open-circuit conditions. *Electrochim. Acta* **47,** 4213–4225 (2002).
30. Wang, P. *et al.* Charge separation and efficient light energy conversion in sensitized mesoscopic solar cells based on binary ionic liquids. *J. Am. Chem. Soc.* **127,** 6850–6856 (2005).
31. Burnside, S. D. *et al.* Self-organization of TiO_2 nanoparticles in thin films. *Chem. Mater.* **10,** 2419–2425 (1998).
32. Ito, S. *et al.* Fabrication of thin film dye sensitized solar cells with solar to electric power conversion efficiency over 10%. *Thin Solid Films* **516,** 4613–4619 (2008).
33. Ito, S. *et al.* Calibration of solar simulator for evaluation of dye-sensitized solar cells. *Solar Energy Mater. Solar Cells* **82,** 421–429 (2004).
34. Ito, S. *et al.* Photovoltaic characterization of dye-sensitized solar cells: Effect of device masking on conversion efficiency. *Progr. Photovol.* **14,** 589–601 (2006).

Acknowledgements

This work was supported by a grant from the Swiss Federal Energy Office (OFEN). The UV-curing glue and the SiO_2 slurry ($d = 600$ nm) were provided by Three Bond (K. Kishi) and CCIC (T. Mizuno and T. Koyanagi), respectively.

Author contributions

S.I. fabricated the TiO_2 electrodes, TiO_2/SiO_2 electrodes and platinum electrodes, assembled cells, and performed the measurements for Figs 2–4. S.Z. synthesized the ruthenium dye (Z907) and the ionic liquid. P.C. synthesized the TiO_2 nanoparticles. P.L. provided guidance on how to assemble the cells and equipment control. D.K. provided the details of the ionic–ionic liquid information. M.G. provided technical advice.

Author information

Reprints and permission information is available online at http://npg.nature.com/reprintsandpermissions/. Correspondence and requests for materials should be addressed to S.I.